5-2002

Phase-space transport of stochastic chaos in population dynamics of virus spread

Lora Billings
Montclair State University, billingsl@montclair.edu

Erik M. Bollt
Clarkson University

Ira B. Schwartz
Naval Research Laboratory

Published Citation

Billings, L., Bollt, E. M., & Schwartz, I. B. (2002). Phase-space transport of stochastic chaos in population dynamics of virus spread. Phys Rev Lett, 88(23), 234101. doi:10.1103/PhysRevLett.88.234101

Phase-Space Transport of Stochastic Chaos in Population Dynamics of Virus Spread

Lora Billings,[1] Erik M. Bollt,[2] and Ira B. Schwartz[3]

[1]*Department of Mathematical Sciences, Montclair State University, Upper Montclair, New Jersey 07043*
[2]*Department of Mathematics and Computer Science, Clarkson University, P.O. Box 5815, Potsdam, New York 13699*
[3]*Naval Research Laboratory, Code 6792, Plasma Physics Division, Washington, D.C. 20375*

(Received 13 September 2001; published 23 May 2002)

A general way to classify stochastic chaos is presented and applied to population dynamics models. A stochastic dynamical theory is used to develop an algorithmic tool to measure the transport across basin boundaries and predict the most probable regions of transport created by noise. The results of this tool are illustrated on a model of virus spread in a large population, where transport regions reveal how noise completes the necessary manifold intersections for the creation of emerging stochastic chaos.

DOI: 10.1103/PhysRevLett.88.234101 PACS numbers: 05.45.–a, 05.10.Gg, 87.23.Cc

In contrast to the notion that noise in physical systems dominated by determinism has small effects, recent research has demonstrated otherwise. Specifically, noise in deterministic dynamical systems plays a prominent role in global behavior due to large-scale effects governed by transport in phase space. Examples of such behavior appear as inducing order in spatiotemporal systems [1], creating phase transitions in wave fronts [2], and excitation of chaoslike structures in large population models, such as lasers [3] and epidemics [4]. These few examples illustrate the general observation that noise may indeed cause a global change in real dynamical systems, thus making it clear that stochastic effects play a definitive role in the dynamics and must be accounted for in our models and our analysis of them. One particular problem is the identification of the cause of qualitatively new emergent dynamics that are not observable in deterministic systems, such as stochastic chaos [4].

In this Letter, we present a general tool designed to predict the global effect of noise on a model of virus spread in a large population. We consider only regions where there is no topological manifold structure for the existence of a chaotic attractor or saddle for noise to excite directly, as in [5]. Our algorithm is designed for the general case of a deterministic dynamical system with several stable basins, called a "multistable" system, in which there is a mixing of states as noise amplitude increases. Since it is not sufficient to compute only Lyapunov exponents to detect or define stochastic chaos [6], we compute transport of a stochastic flux from one basin to another [7,8]. Weighting this flux by the probability density function (PDF) pinpoints regions in phase space that have the greatest leakage into another basin and strongest transport created by noise. This information, combined with the topology of the system, presents a more complete picture of the dynamics, accurately predicting a stochastic bifurcation to new dynamics, such as stochastic chaos. Specifically, we show that stochastic transport correlates quite strongly with the observation that noise completes the correct manifold topology for the existence of stochastic chaos. As such, it also produces the correct statistics to compute both space and time analogs of stochastic Lyapunov exponents.

Some other benefits of our tool are that the dimension of the phase space and the manifold structure are relatively not involved in the stochastic transport analysis. This is in contrast to the way geometric and manifold variation methods, such as the Melnikov method [9], are modified to account for stochastic transport [10]. For these methods, one needs a system to perturb from. Our technique has the advantage that no such "simple" reference system is necessary, as in many population dynamics models. Moreover, our tool is not limited to white noise. It allows for any type of noise perturbation since the distribution of the stochastic perturbations is explicitly defined in the calculation.

We start with a general description of how the tool works. Consider the stochastically perturbed dynamical system

$$F_\nu : M \to M, \qquad x \mapsto F(x) + \eta\,, \tag{1}$$

with the probability density function $\nu(x)$ and a random variable η applied once each iteration. The random part, η is assumed to be independent of state, x, independent identically distributed, which we tacitly presume to be relatively small, so that the deterministic part, F, has primary influence. Noise with a normal distribution is represented by $\nu(x) = \frac{1}{\sqrt{2\pi\sigma^2}} \exp(-\|x\|^2/2\sigma^2)$, with mean $x = 0$ and standard deviation σ as the adjustable parameter. The stochastic Frobenius-Perron operator is

$$P_F[\rho(x)] = \frac{1}{\sqrt{2\pi\sigma^2}} \int_M e^{-\|[x-F(y)]\|^2/2\sigma^2} \rho(y)\, dy\,, \tag{2}$$

which is the form for Eq. (1), a discrete time system with constantly applied stochastic perturbation [11].

Next, we project the infinite-dimensional linear space $L^1(M)$, with discretely indexed basis functions $\{\phi_i(x)\}_{i=1}^{\infty} \subset L^1(M)$ onto a finite-dimensional linear subspace generated by a subset of the basis functions [12], $\Delta_N = \text{span}[\{\phi_i(x)\}_{i=1}^{N}]$, such that $\phi_i \in L^1(M)\ \forall i$. This projection, $p : L^1(M) \to \Delta_N$ is realized optimally by the

"Galerkin" method, in terms of the inner product, which we choose to be integration, $(f,g) \equiv \int_M f(x)g(x)\,dx$, $\forall f, g \in L^2(M)$. Specifically, the infinite-dimensional matrix is approximated by the $N \times N$ matrix,

$$A_{i,j} = (P_{F_\sigma}[\phi_j], \phi_i) = \int_M P_{F_\sigma}[\phi_j(x)]\phi_i(x)\,dx\,, \quad (3)$$

for $1 \le i, j \le N$. One approximates $\rho(x)$ by the finite sum of basis functions, $\rho(x) \simeq \sum_{i=1}^{N} c_i \phi_i(x)$. Choose the basis functions to be a family of characteristic functions,

$$\phi_i(x) = \chi_{B_i}(x) = \begin{bmatrix} 1 & x \in B_i \\ 0 & \text{else} \end{bmatrix}, \quad (4)$$

a nested refinement of boxes $\{B_i\}$ covering M. Therefore, a Galerkin matrix entry, the $A_{i,j}$ value, represents how mass flows from cell B_i to cell B_j, with column sums of one if the space is compact. We wish the A matrix representation to lay plain the regions of transport which leak measure between neighboring basins, across what were transport barriers in the absence of noise. One problem with grid approximations of the phase space is that a typical (say, raster scanned) ordering of the phase space will tend to have those regions that should be dynamically grouped (those in the same basin) scattered seemingly haphazardly in the indexing. Thus, there is a need for reindexing. Our algorithm in brief is to (i) identify vertices corresponding to each basin of attraction in the zero-noise case. (ii) Reindex the corresponding matrix representation $k_1, k_2, \ldots, k_N$ by row/column exchange elementary permutation operations. Further reindex each vertex according to the number of steps to the center of the corresponding basin. (iii) Gradually turn up the noise amplitude while maintaining the zero-noise-determined vertex order, which was previously computed and dynamically coherent. (iv) Identify vertices from which measure leaks, and find their position in the original phase space.

Note that, with no noise, the matrix from a multistable system will completely reduce to a block-diagonal canonical form after reindexing. Adding noise creates nonzero entries in the zero blocks, which correspond to leakage.

There are other quantities which can be easily computed, given the Galerkin matrix A. The dominant eigenvector of A approximates the invariant PDF of the dynamical system. Such a spatial integration, which is essentially an Ulam method [13], is the straightforward alternative to the direct but often less efficient method of time verages involving accumulating histograms over long orbits [9]. Given (approximately) the invariant PDF, we can approximate the Lyapunov exponents, also by direct spatial integration. Let $\rho(x)$ be the PDF and $\{\lambda_k(x)\}$ be the eigenvalues of the Jacobian evaluated over one time period, starting at an initial condition x. Lyapunov exponents can be computed by spatial averaging against the invariant PDF, which our numerical experiments suggest perfect agreement with time average computation

$$\Lambda_k = \int_M \ln \|\lambda_k(x)\| \rho(x)\,dx\,. \quad (5)$$

Note that the eigenvalues $\{\lambda_k(x)\}$ of $F(x)$, the deterministic part of Eq. (1), are independent of the properties of the stochastic perturbations η. Since the PDF changes with the standard deviation of noise, so do the Lyapunov exponents, but the calculation of Eq. (5) remains straightforward since $\{\lambda_k(x)\}$ remains fixed. We call the measurement of a positive Lyapunov exponent an indicator of stochastic chaos. This condition is necessary but not sufficient, and the apparent geometry of the stable and unstable manifolds under the influence of noise is another strong indicator of chaoslike behavior.

Given a region, it is possible to define *mass flux* (or simply flux) in and out of the region, across the boundary [14]. To approximate flux, say, for cell i in Basin 1, we calculate the absolute sum of all columns j of $A_{i,j}$ corresponding to Basin 2. The flux for each ith region can be weighted to form masked transfer matrices. Choosing an initially uniform density, we can find stochastic *area flux.* Using the PDF weighting corresponds to the joint probability that a trajectory visits a region by the probability of the trajectory escaping from that region. We call this the *PDF flux,* which pinpoints regions in phase space that have the greatest leakage into another basin.

To illustrate the methodology described above, we consider a model used to describe the dynamics of virus spread in a large population. In [4] it was shown that, when noise with a sufficiently large standard deviation is added, the behavior of the modified SI (MSI) model [15,16],

$$\begin{aligned} S'(t) &= \mu - \mu S(t) - \beta(t) I(t) S(t)\,, \\ I'(t) &= \left(\frac{\alpha}{\mu + \gamma}\right)\beta(t) I(t) S(t) - (\mu + \alpha) I(t)\,, \\ \beta(t) &= \beta_0(1 + \delta \cos 2\pi t)\,, \end{aligned} \quad (6)$$

was transformed from regular, periodic cycles to something completely different, which we call stochastic chaos. In the deterministic case, with parameter values at $\mu = 0.02$, $\alpha = 1/0.0279$, $\gamma = 100$, $\beta_0 = 1575$, and $\delta = 0.095$, there exist two stable periodic orbits, two unstable periodic orbits, and a partially formed heteroclinic orbit. The newly developed a tool in this Letter pinpoints the flux between basins as noise is added. Multiplying these rates by the probability density function results in the measure of where a trajectory is most likely to escape to another basin. We find that the highest escape rates occurs exactly where we previously conjectured, at the near heteroclinic tangencies, thus creating a chaoslike orbit.

Without noise, trajectories starting in the neighborhood of the stable period-two or period-three orbits simply converge to one of these two attractors. Since Eq. (6) is driven by a time-periodic function $\beta(t)$, and both S and I are fractions of the population, we can integrate to a stroboscopic map between unit boxes,

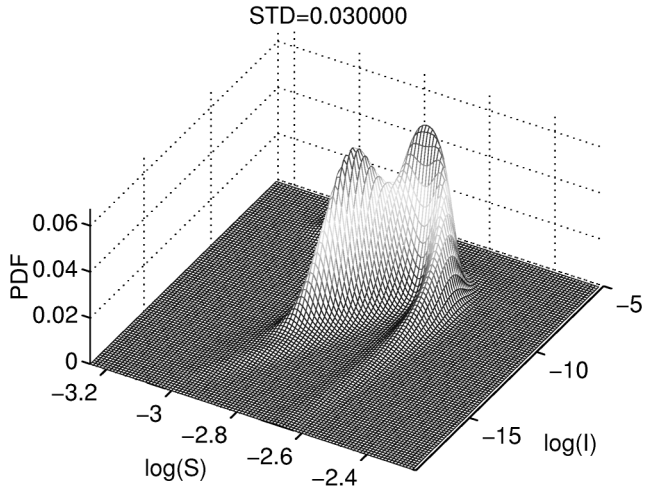

FIG. 1. The PDF of the MSI model for the standard deviation $\sigma = 0.03$ calculated as the dominant eigenvector of the Galerkin matrix.

$F[0,1]^2 \to [0,1]^2$. In keeping with the assumed form of Eq. (1), a discrete time system with constantly applied stochastic perturbation, we add Gaussian noise directly to the population rate equations, discretely at each strobe of the map. We solve the deterministic part of the map F by a numerical ordinary differential equation solver of our choice to find the solution during the time the trajectory is off the Poincaré section, and then we add Gaussian noise of mean zero, and standard deviation σ on the section. Continuously added noise must be accounted for by a Langevin equation, with a corresponding Fokker-Planck–type equation, which continuously evolves in time initial density profiles [11]. We add noise discretely on the stroboscopic section, in this case using the assumed Gaussian form, corresponding to a continuously added noise of another distribution [17].

We now propose the mechanism behind the noise-induced transport of the MSI model by applying our above-described tools, essentially as a black box. Following the algorithm requires little special consideration for our specific system. Once we have raster scanned an index to cover the attractor by a coarse grid, the resulting Galerkin matrix approximation of the Frobenius-Perron operator is essentially dimension independent, with no memory of the phase space from which it was formed.

In Fig. 1 for $\sigma = 0.03$, we see the invariant density or PDF of the MSI model. This picture is calculated as

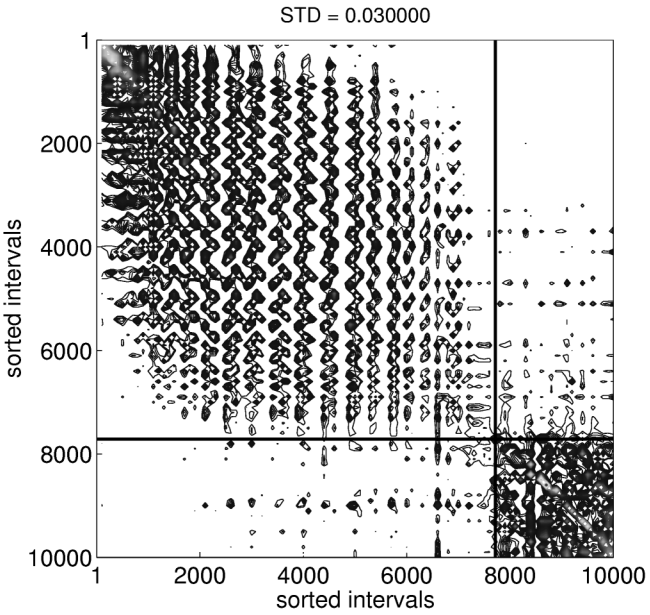

FIG. 2. The sorted Galerkin matrix for the standard deviation $\sigma = 0.03$. The grid points in the period-two basin are sorted to the left, and the period-three points are on the right, divided by the black line. The top left and the bottom right blocks represent the dynamics within the basins, while the bottom left and top right represent the leakage from one basin to another.

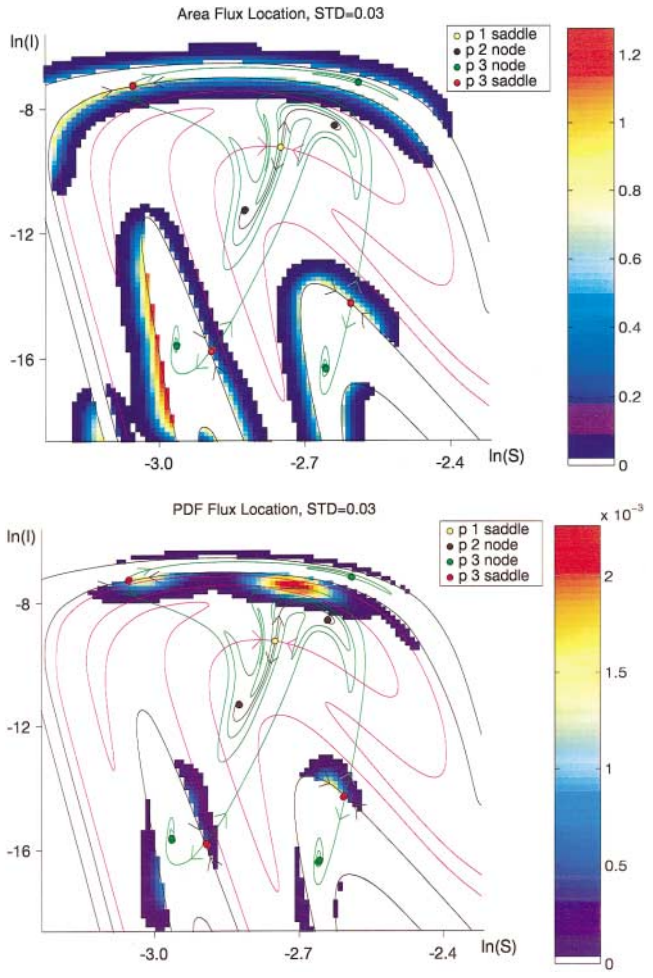

FIG. 3 (color). The area flux (top) and PDF flux (bottom) over the phase space for the period-two basin (left). The periodic orbits are indicated by the large colored dots. These graphs show the regions where trajectories escape to the period-three basin. The colors indicate the relative rates varying from the greatest (red) to the least (blue). Notice that the greatest flux happens along the basin boundaries.

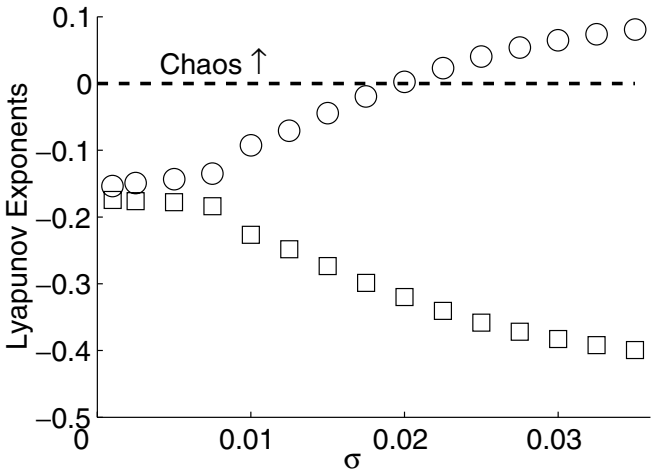

FIG. 4. The Lyapunov exponents as a function of the standard deviation (σ) found by evaluating Eq. (5). The maximum Lyapunov exponent crosses zero near $\sigma = 0.02$, indicating the onset of stochastic chaos.

the dominant eigenvector of the corresponding Galerkin matrix. The essential feature is that, when $\sigma = 0$, the two main density spikes are at the dynamic centers of each respective basin. Initially, as σ increases, the density becomes less diffusely distributed around the stable fixed points, due to the predominantly small stochastic diffusion added to the deterministic dynamics. There persist two stable fixed points and two distinct basins. As we continue to increase σ, a crossover effect occurs near $\sigma = 0.02$, after which the density mass becomes mixed throughout a larger region and predominantly mixed between the originally separate basins.

In Fig. 2, we see a sorted matrix for $\sigma = 0.03$. The bistable system completely reduces to a canonical two-block diagonal form when $\sigma = 0$. By using this reindexing instead of the original spatial coordinates, we see clearly the cause of the density that leaks between the formerly separate basins: there is a loss of reducibility of the corresponding (here approximated) operator. With the measurement of PDF flux, we can find the locations with the most transport. In Fig. 3, we show both the area and PDF fluxes for leakage from the period-two to period-three basin when $\sigma = 0.03$. We see "pretangency" mixing: the PDF flux reveals that the greatest transport occurs where the unstable manifold of the period-one saddle is closest to the stable manifold of the period-three saddle, thus essentially completing the heteroclinic tangle. Checking the Lyapunov exponents, $\Lambda_1 = 0.1294$, $\Lambda_2 = -0.7658$, confirms the noise-induced, or stochastic, chaoslike behavior. Figure 4, a graph of the Lyapunov exponents as a function of the standard deviation, indicates the onset of stochastic chaos near $\sigma = 0.02$. Note that there is good agreement between the spatial integration-based computation in Fig. 4 and a similar graph based on time averaging and histograms found in [4].

In conclusion, we have described a new tool that computes stochastic transport in a population dynamics model without necessarily requiring the existence of a chaotic repeller. The tool uses a Galerkin projection of the Frobenius-Perron operator, which describes the mass flow from cell to cell. This allows us to determine the mass flux across basin boundaries, the probability density function, and the Lyapunov exponents using spatial information and as an alternative to time averaging. This information, combined with the topology of the system, accurately predicts the stochastic bifurcation to new dynamics, pinpointing the changes caused by the addition of noise as illustrated by the noise-induced chaos in the MSI model. The method is generic to any dynamical system with any type of stochastic perturbations, making it a powerful tool to predict the unexpected effects of noise.

I. B. S. is supported by the Office of Naval Research. L. B. is supported by the Office of Naval Research N00173-01-1-G911. E. M. B. is supported by the National Science Foundation under Grant No. DMS-0071314.

[1] J. García-Ojalvo and J. M. Sancho, *Noise in Spatially Extended Systems* (Springer-Verlag, New York, 1999).
[2] S. Kadar, J. Wang, and K. Showalter, Nature (London) **391**, 770 (1998).
[3] J. Gao, S. Hwang, and J. Liu, Phys. Rev. A **59**, 1582 (1999).
[4] L. Billings and I. Schwartz, J. Math. Biol. (on-line publication: 12/7/2001).
[5] J. Crutchfield, J. Farmer, and B. Huberman, Phys. Rep. **92**, 45 (1982).
[6] D. A. Rand and H. B. Wilson, Proc. R. Soc. London B **246**, 179 (1991).
[7] M. Dellnitz and O. Junge, SIAM J. Numer. Anal. **36**, 491 (1999).
[8] R. Courant and D. Hilbert, *Methods of Mathematical Physics* (Wiley, New York, 1970), Vol. 1.
[9] S. Wiggins, *Chaotic Transport in Dynamical Systems* (Springer-Verlag, New York, 1992).
[10] E. Simiu, J. Appl. Mech. **63**, 429 (1996).
[11] A. Lasota and M. C. Mackey, *Chaos, Fractals, and Noise* (Springer-Verlag, New York, 1994), 2nd ed.
[12] T. Y. Li, J. Approx. Theory **17**, 177 (1976).
[13] F. Hunt, J. Math. Anal. Appl. **198**, 534 (1996).
[14] E. Bollt, Ph.D. thesis, University of Colorado, Bolder, 1995.
[15] I. Schwartz, J. Math. Biol. **21**, 347 (1985).
[16] I. Schwartz, J. Math. Biol. **30**, 473 (1992).
[17] The continuous semigroup of solutions to the Fokker-Planck partial differential equations, with an assumed noise distribution, generates a discretely indexed subsemigroup which evolves discrete densities under an added noise of another (accumulated) noise distribution [11].